Assessment of the Sub-Base Material for the Optimum Moisture Content and Maximum Dry Density Using Amalgamated Pond Ash with Reclaimed Asphalt on Road Pavement

Radhakrishnan Vijayakumar[1*], Kumar Govidhasamy[1]

[1] Department of Civil Engineering, Vel Tech Rangarajan Dr. Sagunthala R&D Institute of Science and Technology, Avadi, Chennai, 600 062, India

* Corresponding author's e-mail: vtd747@veltech.edu.in

ABSTRACT

The subgrade is a crucial part of the pavement structure, as it transmits the load of vehicles on the pavement to the subsoil. The stability of the pavement depends on the stability characteristics of the subgrade. Roadwork waste materials (RWM) constitute a significant portion of waste materials used for roadway construction, particularly in base fill and backfill layers. Due to the shortage of virgin raw aggregates from quarries, alternative materials, such as RWM, are used as replacements in regular roadway construction. This research conducted a wide range of laboratory and field evaluations to determine the engineering properties of pond ash (PA) and reclaimed asphalt pavement (RAP), focusing on bottom ash as a blended material. Geotechnical parameters, such as particle size and mechanical properties of the materials, were assessed to evaluate their performance in pavement base or sub-base applications. The interaction of integrity between pond ash, RAP, and natural backfill as homogeneous materials was assessed by examining consistency characteristics concerning optimum moisture content (OMC) and maximum dry density (MDD). Six proportions of pond ash, RAP, and backfill soil (PA, RAP, NBS) were identified and used, with the optimal proportion being 50%:30%:20%. The grain size of RAP required for soil testing suitability will be obtained by disintegration using an earth hammering machine.

Keywords: pond ash; asphalt; maximum dry density; optimum moisture content; sub-grade.

INTRODUCTION

India's road network spans over 5.9 million kilometers, making it the second-largest road network in the world, surpassed only by the United States. The majority of road surfaces are bituminous and require regular maintenance work. The rehabilitation or resurfacing process produces large quantities of reclaimed asphalt pavement (Dager et al., 2023). With the tremendous consumption of coal as a fossil fuel to meet the demands of daily life (Qin et al., 2023), significant amounts of pond ash accumulate every day. Disposing of industrial waste and its by-products is becoming increasingly difficult and costly. Both flexible and rigid road pavement constructions consume large quantities of aggregates and binders, making the preservation of natural resources

an important issue (Zhang and Yang 2021). The use of reclaimed asphalt pavement (RAP) in mixtures has increased in recent years, as it reduces the demand for virgin materials, such as aggregate and asphalt binder, protects natural resources, and lowers construction costs (Zhang and Yang 2022). Incorporating RAP in hot mix asphalt (HMA) minimizes the waste material disposal costs in existing pavement. The addition of RAP in HMA has become more commonplace worldwide, with numerous studies and literature focusing on the advantages, disadvantages, and optimal ratios of recycled materials (Barmade et al., 2022). The use of RAP in highway construction aligns with the global objective of sustainable growth through the efficient utilization of natural resources. Incorporating pond ash was proven by (Gupta and Kumar 2016; Karthikeyan

et al., 2017). The reclaimed asphalt pavement materials as aggregates in flexible road construction and soil stabilization for roads and other types of construction can reduce environmental stress and the exploitation of natural resources (Rout et al., 2023; Plati et al., 2022). Granular sub-base material (GSB) is recommended as a matrix material suitable for bridge work and road works. According to IS: 2720, coarse-graded sub-base granular materials can be used if they pass through a 425 – micron sieve. The Indian Road Congress mandates the distribution of specified grain sizes for the sub-base material to meet strength and drainage requirements. The effectiveness of highway pavement structural design primarily depends on the accuracy and evaluation of materials (Liu et al., 2021; Liu et al., 2022). Pond ash, a waste by-product of coal burning, is abundant at sites such as the Ennore Thermal Power Plant Station in Ennore, Tamil Nadu. The estimated volume of pond ash (fly ash) deposition in the area is 3,983,002 cubic meters (approximately 5.67 million metric tonnes), with 1,911,830 cubic meters (approximately 2.67 million metric tonnes) present in the backwaters and the remaining in the flood plains. In roadway construction, compaction (Zhang et al., 2019; Kaseer et al., 2019). The water content and dry unit weight serve as reference parameters for optimum water content and maximum dry density, conforming to specific compaction techniques (Sarkar and Dawson 2017). Reprocessing pavement materials has become essential for sustainable road rehabilitation and maintenance. Resource conservation, environmental preservation, and retaining existing geometrics are advantages of reusing pavement materials. The performance of RAP has been assessed through construction projects worldwide (Pasandín and Pérez 2013). Field performance comparisons and evaluations show that RAP is a suitable material, providing higher dry density than conventional granular materials. Mixing and heating are considered to improve RAP properties and minimize creep. As RAP temperature increases, stiffness and strength increase as well. The primary application of RAP is as a structural fill, with construction activities recommended during the summer months. The line-of-optimums is used for compaction monitoring to estimate the optimum water content and/or maximum dry unit weight of cohesionless soil. Recycled and reused materials are typically employed under non-acidic environmental conditions. Moreover, the chemical leaching of RAP

varies across different studies. The RAP chemical composition depends primarily on its use, exposure over time, and source. Research suggests that RAP does not pose significant leaching threats when used as fill, provided it is not employed near water sources or as embankment materials (Muniamuthu et al., 2022). There is a need to develop a generic hot recycled asphalt plant mix featuring densely graded bituminous mixes suited to Indian standards. This ensures that RAP can be used for resurfacing and/or new bituminous pavement construction (Yang et al., 2022). This development is being considered by the Flexible Pavement Committee (FPC) of the Indian Road Congress (IRC 120: 2015). Research on RAP material has increased worldwide, as it exhibits versatile and adaptable geotechnical properties for pavement. The variability of RAP necessitates synthesizing existing data, identifying recent gaps, and recognizing the areas for further research. A comprehensive review of the literature investigates the geotechnical properties of RAP. By compiling the RAP geotechnical properties from around the world, the study suggests that the reuse of waste materials extends beyond pavement applications. The RAP engineering properties are assessed, providing recommendations for its use as a viable alternative in highway transportation infrastructure engineering applications. Many young researchers tried the work concerning the pond ash (PA) and RAP subjected to the mixing of flitched materials and other binders with maximum proportions of 50% PA and 50% flitched materials combined with rock salt materials; however, there are no studies on limited constraints of pure pond ash as base material followed by 50%:30%:20% proportions. The main objective of this study was to determine the optimum value of moisture content and maximum dry density of the mixed proportions of PA, RAP, and natural backfill soil. In the experimental study, maximum dry density (MDD) and optimum moisture content (OMC) increased with the decreasing mix proportions of PA from 90 to 50%, RAP from 50 to 30%, and natural backfill soil from 50 to 20%. The novelty of this work is adding the limited constraints with pure pond ash improving the quality of OMC and MDD. This gives the extreme mechanical behavior of this proportions than other conventional results. One more novelty and challenge in this research is utilizing the asphalt binder with limited proportions improving the surface properties and excellent reinforced properties compared to other

conventional methods. The penetration, viscosity grades, ductility, softening points, and desirable mechanical properties of these proportions for PA and RAP concerned with 50%:30%:20% proportions have been completely improved. This motivational research gives challenging ideas for young researchers who are willing to obtain interesting results from concrete, pond ash, and other binders, including mechanical strength, reinforced strength, and other properties. The cost adopted for this research is also low and very eco-friendly for construction purposes.

MATERIALS AND METHODS

Asphalt pavement materials are commonly found and removed during restoration, resurfacing, or renovation operations. Once removed and processed, these materials become RAP, which contains valuable aggregate and asphalt binder. Three materials are typically utilized in this context.

Bitumen

When the quantity of RAP in the recycled hot bituminous mix is 20% or less, the viscosity grade of bitumen should be the same as specified in Table 1. If the quantity of RAP in the mixture ranges from 20 to 35% (Seferoğlu et al., 2018). The viscosity grade of the virgin bitumen should be one grade softer than the grade generally specified for a 100% virgin mix. For instance, if VG – 20 grade is used in the recycled mix, VG – 30 would be selected for a 100% virgin mix. If the amount of RAP exceeds 30%, the viscosity grade of the virgin bitumen used in the recycled mix should be determined using the blending chart provided in ASTM D 4887. However, under no circumstances should the selected viscosity grade

be more than two grades softer than the grade typically used in the project (Kumar et al., 2024; Al-Ghurabi and Al-Humeidawi 2021).

Reclaimed asphalt pavement material

RAP should be obtained from a uniform stockpile created through cold milling or crushing hot bituminous mixes sourced from similar bituminous courses of existing bituminous pavement (Pradhan and Biswal 2022). Table 2 shows the physical and mechanical properties of the RAP used in this research. The RAP material should be free of foreign materials and exhibit minimal segregation. RAP should be processed so that the final recycled mix meets all requirements of the specific mix as outlined in IRC: 111-2009 (Edeh et al., 2019). During the hot mixing process, RAP should readily break down and blend with the virgin materials without affecting the paving operation. At least 95% of the RAP material should pass without impacting the paving operation (Saravanan et al., 2024). If the maximum size of the aggregate in RAP exceeds the maximum size of the aggregate in the specified recycled mix, additional sizing and crushing will be required (Tarsi et al., 2020).

Reclaimed aggregate material (RAM)

RAM shall meet all the applicable requirements of coarse and fine aggregates as specified in Sections 3.2 and 3.3 of IRC: 111–2009.

EXPERIMENTAL INVESTIGATIONS

Composition of mixtures

The composition of recycled bituminous mix (bitumen content and gradation) shall comply with the composition of 100% virgin mix as specified in Section 3.5 of IRC: 111–2009.

Table 1. Bitumen VG-30 specifications

S. No.	Description	Method	VG-30
1	Penetration at 250 °C, 100 gm, 5 s, 0.1 mm, min		45
2	Absolute viscosity at 600 °C, poise	IS:1206 (part 2)	2300–3500
3	Kinematic viscosity at 135 °C, cSt, min	IS:1206 (part 3)	345
4	Flash point (cleveland open cup), °C, min	IS 1448	210–220 °C
5	Solubility in trichloroethylene, % min	IS 1216	97–99
6	Softening point, °C, min	IS 1205	44
7	Viscosity ratio at 60 °C	IS:1206 (part 2)	4
8	Ductility at 25 °C	IS 1208	38

Table 2. Physical and mechanical properties of reclaimed asphalt pavement

Type of property	Description	Appropriate **v**alues
Physical properties	Unit weight	18.633 to 22.55 kN/m³
	Moisture content	nominal: 5% maximum: 8%
	Asphalt content	4.5 to 8%
	Asphalt penetration	20 to 60 at 25 °C
	Recovered asphalt cement	3000 to 20,000 poises
Mechanical properties	Compacted unit weight	15.7 to 21 kN/m³
	California bearing ratio	100% RAP: 30–45% 50% RAP: 20–30% 25% RAP: 10–15%

Design of recycled mixes

The design of the hot recycled mix should adhere to Section 4 of IRC: 111–2009, except for the following deviations. The total amount of RAP in the recycled mix should be limited to 25% in the wearing course and 50% in binder and base courses. These limits of 25% for wearing courses and 50% for binder and base courses are reasonable for India. At least five random samples of RAP should be obtained from the approved RAP stockpile for conducting extraction tests to determine the average bitumen content (Kumar et al., 2023). The average gradation of aggregates in RAP. When determining the blending proportions of various aggregates, the extracted aggregate should be considered as one of the aggregates. This process requires extraction and recovery of aged bitumen from the RAP from at least three random samples of the RAP from the stockpile. Bitumen should be extracted according to ASTM D 2172, which outlines the quantitative extraction of bitumen from bituminous paving mixtures. A list of experimental tests that can be carried out for the blended mixture includes specific Gravity, direct shear tests, consistency limits, compaction tests, grain size analysis (mechanical and sedimentation), and unconfined compression tests (Antunes et al., 2021).

Sampling of material

PA is sourced from Ennore Thermal Power Plant, Tamil Nadu, while the RAP is obtained through milling old road surfaces and backfilling from the local roadside of ORR Chennai. These materials are combined to form a unique matrix sample. The sample is dried in a kiln at 105–110 °C. Subsequently, the resultant material is sieved using a 2 mm sieve. The material that passes through the 2 mm sieve is then used in the experimental work (Gottumukkala et al., 2018).

Determination of index properties

Specific gravity of the pond ash

PA specific gravity is determined according to IS 2720 part 3 (1980) as shown in Figure 1 and the value was obtained as 2.29.

Determination of grain size Distribution-IS 2720-4 (1985)

Methods of testing for soils are as follows: 1 kg of pond ash sample is washed thoroughly and allowed to pass via sieve sets in descending order (Figure 1). Then, the percentage weight retained in each sieve is recorded and the corresponding values are calculated and shown in Table 3.

Determination of fineness modulus

To determine the fineness modulus, the matrix of 15 kg is obtained and sieved thoroughly from an IS sieve size of 150 microns. A sample of 15 kg was obtained for analysis as represented in Table 4.

Determination of resilient modulus

The resilient modulus (MR) indicates the stiffness of a sub-grade material. The resilient modulus of a material measures its elasticity, calculated by dividing the stress by strain for rapidly applied loads, which are typically experienced by pavements. The resilient modulus can be estimated using the triaxial test. This test applies a repetitive axial cyclic load with fixed magnitude, load duration, and cyclic frequency to a cylindrical test specimen. The specimen

Figure 1. The specific gravity of PA and grain size analysis of pond ash

Table 3. Pond ash in sieve analysis

Sieve size (mm)	Weight of retained particles (gm)
10.00	0
4.750	0
2.000	115
1.180	210
0.600	195
0.300	206
0.150	187
0.075	78
Pan	–
Total	991
Weight loss	(1000−991)/1000 × 100 0.9% – less than 2%

$$M_r = \frac{\sigma_d}{\varepsilon_r} \qquad (1)$$

where: σ_d is the deviator stress, and ε_r is the recoverable elastic strain.

According to IRC 37: 2012, the relation between resilient modulus and the effective CBR is given by proportions as mentioned in Table 5. Eq. 2 and Eq. 3 represent the resilient modulus concerning CBR ratios.

$$M_r = 10 \times \text{CBR}; \text{ for CBR } \leq 5 \qquad (2)$$

$$M_r = 17.6 \times \text{CBR}^{0.64}; \text{ for CBR } > 5 \qquad (3)$$

Since the CBR ratio is greater than 5; therefore, the resilient modulus is

$$M_r = 17.6 \times 9.120.64 = 72.43\text{pa} \qquad (4)$$

The M_r value for the optimum mixture is 72.43 MPa, which is very close to 75 MPa as recommended by IRC: 37:2012, for a pavement thickness of approximately 500 mm.

is subjected to dynamic cyclic and static confining stress provided by a triaxial pressure chamber. Essentially, it is a cyclic variation of a triaxial compression test, in which the cyclic load application is designed to simulate actual traffic loading accurately. Resilient modulus (M_r) is represented in Eq. 1

Table 4. Sieve analysis of mixture

Wt. of retained particles in the sieve			
IS sieve size (mm)	Wt. retained (kg)	% of cumulative weight retained (kg)	Cumulative retained (%)
20	1.52	–	10.133
10	3.28	4.80	32.000
4.75	6.347	11.147	74.310
2.36	2.124	13.271	88.473
1.18	1.172	14.443	96.286
0.6	0.304	14.747	98.313
0.3	0.140	14.887	99.246
0.15	0.075	14.962	99.750
Pan	0.005	14.967	99.780
Total			698.291
Fineness modulus			6.98

Table 5. Calculation of CBR values for all mix proportions

Description	Specimen 1		Specimen 2		Specimen 3		Specimen 4		Specimen 5		Specimen 6	
	2.5 mm	5 mm	2.5 mm	5 mm	2.5 mm	5 mm	2.5 mm	5 mm	2.5 mm	5 mm	2.5 mm	5 mm
Proving ring reading	84	102	77	93	79	99	80	103	88	109	83	95
Factored load (kg) A	84 × 1.42 = 119.28	102 × 1.42 = 144.84	77 × 1.42 = 109.34	93 × 1.42 = 132.06	79 × 1.42 = 112.18	99 × 1.42 = 140.58	80 × 1.42 = 113.6	95 × 1.42 = 134.9	88 × 1.42 = 124.96	97 × 1.42 = 137.74	83 × 1.42 = 117.86	95× 1.42 = 134.9
Std load (kg) B	1370	2055	1370	2055	1370	2055	1370	2055	1370	2055	1370	2055
CBR ratio A/B × 100 (%)	8.71	7.0	7.98	6.43	8.2	6.84	8.29	7.12	9.12	7.53	8.6	6.56
Optimum CBR ratio	2.5 mm penetration = 9.12%											
	5 mm penetration = 7.53%											

Determination of engineering parameters

Experimental investigation is carried out according to IS 4332-3:1967 to estimate the blended sample's moisture content. In addition, dry density through a compaction test setup complies with IS 4332-3:1967 for pond ash, and for mixture IS 2720-7:1980, the OMC and MDD relation is adopted (Ghanizadeh et al., 2018) represented in Table 6.

Analysis of shear parameters – direct shear test according to IS 2720-13:1986

The experimental procedure is conducted through direct shear tests in geotechnical engineering practice and research to determine the soil shear strength characteristics as represented in Table 7. Shear parameters, such as cohesive strength and angle of internal friction, were determined by maintaining a varied moisture content and a constant maximum dry density (Elkashef et al., 2019; Sunil Kumar et al., 2022). Other cases include maintaining optimum moisture content as constant and dry density as variable. Tables 8 and 9 illustrate the results of different standards.

Determination of unconfined compressive strength using unconfined compression test

According to IS 2720-10:1991, experiments were performed on unreinforced specimens. Compressive strength was found for different compactions, fixed densities, and moisture contents as represented in Tables 10 and 11. Table 12 represents the maximum dry densities. Maximum dry density and moisture content relation determination for the mixture soil is tabulated below.

Table 6. Compaction characteristics for blended pond ash, RAP, and local soil backfill

S. No.	Compaction energy (kg-cm)	OMC in %	MDD in kN/m³	Degree of saturation
1	3576	36.43	15.6	0.880
2	5995	33.56	15.87	0.833
3	15.114	30.67	15.96	0.812
4	26.893	29.65	16.46	0.796
5	27.897	28.45	16.76	0.785
6	34.567	28.22	7.12	0.781

Table 7. Shear parameters for different compaction efforts for pond ash

S. No	Compaction effort (N-m)	Dry density (kN/m³)	Moisture content (%)	c (kg/cm²)	Φ (degree)
1	350.7	15.60	36.43	0.153	21.90
2	587.9	15.87	33.56	0.105	20.81
3	1482.2	15.96	30.67	0.116	21.80
4	2637.3	16.46	29.65	0.116	23.94
5	2735.8	16.76	28.45	0.079	20.81
6	3389.9	7.12	28.22	0.100	23.75

Table 8. OMC standard proctor

S. No.	Moisture content (%)	Dry density (g/cc)	Φ (degree)	c (kg/cm²)
1	55.91	1.10	13.62	0.0479
2	45.92	1.10	14.57	0.0288
3	25.91	1.10	15.82	0.0216
4	20.91	1.10	15.81	0.0024

Table 9. OMC subjected to 28.3% and modified proctor MDD

S. No.	Type of experiment	Dry density (g/cc)	Moisture content (%)	Compressive strength (N/cm²)	Compressive strength (N/cm²)
1	Standard proctor	1.10	35.91 + 10	0.158	1.58
2		1.10	35.91 − 10	0.700	7.00
3	Modified proctor	1.24	28.30 + 10	0.500	5.00
4		1.24	28.30 − 10	2.500	25.0

Table 10. Compressive strength is related to compaction effort

S. No.	Dry density (g/cc)	Moisture content (%)	Φ (Degree)	c (kg/cm²)
1	1.24	48.30	13.73	0.0455
2	1.24	38.40	14.72	0.0431
3	1.24	18.40	14.17	0.0046
4	1.24	13.30	17.83	0.0264

Table 11. Compressive strength for MDD constant and variable moisture content

S. No.	Compaction energy (N-m)	Compressive strength (N/cm²)	Compressive strength (kN/m²)
1	356.9	0.112	1.12
2	594.8	0.471	4.71
3	1492.9	0.589	5.89
4	2673.3	0.952	9.52
5	2789.4	1.010	10.10
6	3486.7	1.167	11.67

Eq.5. represents compaction curves respected to dry and wet moistures. Eq. 6. represents densities of mixtures, and Eq. 7. represents dry density fractions.

1. Calculation of compaction curve

$$W_s = W_m - W_{ms} \qquad (5)$$

where: the weight of compacted soil in grams is W_s, the weight of mold with base plate and without collar is W_m, the weight of mold with compacted soil is W_{ms}, the volume of the mold is $v = 1000$ cc, and water content is w.

2. Bulk density in gm per volume (ρ)

$$\rho = \frac{W_s}{v} \qquad (6)$$

3. Dry density (ρ_d)

$$\rho_d = \frac{\rho}{(1+w)} \qquad (7)$$

RESULTS AND DISCUSSION

Modified Proctor compaction and standard Proctor compaction tests were conducted for various mixes, ranging for PA from 90 to 50%. In contrast, RAP materials and natural backfill soil ranged from 50% to 30%. Characteristics, such as bulk density, dry density, and moisture content, were determined for all the ratios, and the optimum values were obtained from the results. A graphical representation is used to plot maximum

Table 12. Max. dry density moisture content relation according to IS 2720-8

S.No.	Description	No. 1	No. 2	No. 3	No. 4	No. 5
Specific gravity of soil mixture = 2.64
Volume of mould = 1000 cc or 1000 mL
Wt. of empty mould = 2246 g			Sample number			
Sample type = Mix 1 (0.9:0.5:0.5) pond ash: RAP: natural backfill soil
1	Wt. of mould + compacted soil	4329	4458	4663	4643	4420
2	Wt. of compacted soil	2083	2212	2417	2397	2174
3	Bulk density	2.08	2.21	2.42	2.39	2.17
4	Water content	7.53	8.40	10.15	11.70	14.12
5	Dry density	1.92	2.04	2.19	2.14	1.91
Sample type = Mix 2 (0.8:0.1:0.1) pond ash: RAP: backfill soil, wt. of empty mould = 4224
1	Wt. of mould + compacted soil	6199	6336	6438	6440	6373
2	Wt. of compacted soil	1975	2112	2214	2216	2149
3	Bulk density	1.975	2.112	2.214	2.216	2.149
4	Water content	4.33	6.03	8.5	10.42	12.42
5	Dry density	1.893	1.992	2.041	2.007	1.912
Sample type = Mix 3 (0.7:0.2:0.1) pond ash: RAP: backfill soil, wt. of empty mould = 4810
1	Wt. of mould + compacted soil	6726	6850	6960	6940	6850
2	Wt. of compacted soil	1916	2040	2150	2130	2040
3	Bulk density	1.92	2.04	2.15	2.13	2.04
4	Water content	8.0	9.5	10.8	12.5	14.0
5	Dry density	1.78	1.86	1.94	1.89	1.79
Sample type = Mix 4 (0.6:0.2:0.2) pond ash: RAP: backfill soil, wt. of empty mould = 4224
1	Wt. of mould + compacted soil	7567	7732	7965	8186	8160
2	Wt. of compacted soil	3343	3508	3741	3962	3936
3	Bulk density	1.572	1.649	1.759	1.863	1.850
4	Water content	8.5	9.1	10.1	11.2	12.5
5	Dry density	1.449	1.509	1.598	1.675	1.644
Sample type = Mix 5 (0.5:0.3:0.2) pond ash: RAP: backfill soil, wt. of empty mould = 4810
1	Wt. of mould + compacted soil	6738	6838	6875	6971	6945
2	Wt. of compacted soil	1928	2028	2065	2161	2153
3	Bulk density	1.928	2.028	2.065	2.161	2.153
4	Water content	5.15	7.55	8.87	11.7	12.14
5	Dry density	1.834	1.886	1.897	1.935	1.925
Sample type = Mix 6 (0.4:0.3:0.3) pond ash: RAP: backfill soil, wt. of empty mould = 4810
1	Wt. of mould + compacted soil	6557	6628	6746	6723	6738
2	Wt. of compacted soil	1747	1818	1936	1913	1928
3	Bulk density	1.747	1.818	1.936	1.913	1.928
4	Water content	5.5	7.66	9.5	12.4	14.2
5	Dry density	1.656	1.689	1.768	1.702	1.688

dry density versus optimum moisture content, allowing for determining the optimum moisture content and maximum dry density under different sampling conditions (Bishnoi 2023). Figure 2 illustrates the moisture content at 10.45% and dry density at 2.17 g/cc for the mix proportion of 90% pond ash, 5% RAP, and 5% backfill soil. On the dry side, the plot has three variable points, which

between the dry and wet sides, with a steady increase in dry density before and after 100% compaction (Srimanickam and Kumar 2021). When the proportion of RAP and backfill is increased, irrespective of mix 2, to maintain the unit volume, the MCC exhibits an incremental scale of 25%, and dry density decreases by 5.7% in the ratio of 0.23 for maximum moisture content to dry density (Arshad and Ahmed 2017). Figure 5 presents a regularized parabolic curve, displaying the
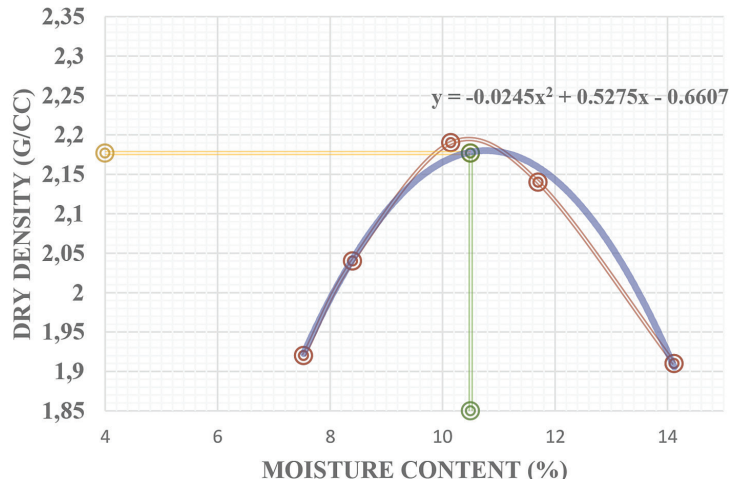

$$y = -0.0245x^2 + 0.5275x - 0.6607$$

Figure 2. Dry density vs. moisture content for sample mix type 1
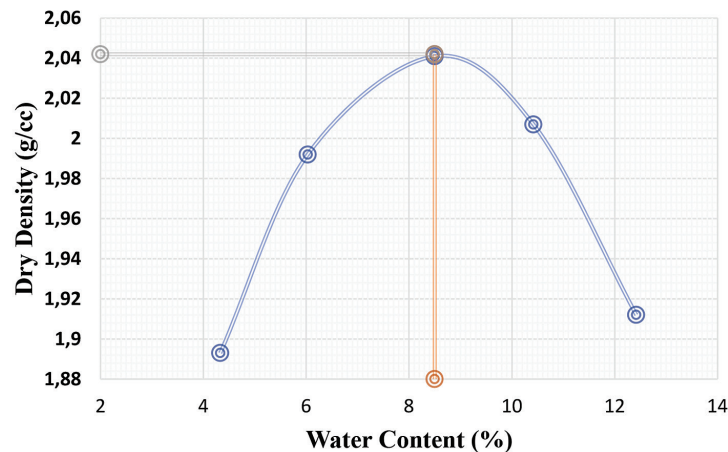
Figure 3. Moisture content vs. dry density for sample mix type 2

exhibit an apparent exponential rise compared to the wet side, which has two variable points that display a more comprehensive extension after 100% compaction (Adhikari et al., 2020). This finding indicates that increasing the proportion of RAP or backfill soil is not advisable. Therefore, iterations can be performed with decremented values of mix proportion, using sample mix type 1 as a reference mix. Figure 3 illustrates the moisture content at 8.45% and dry density at 2.046 g/cc for the mix proportion of 80% pond ash, 10% RAP, and 10% backfill soil. Figure 3 displays the symmetry plot between the dry and wet sides

after 100% compaction. When the proportion of RAP and backfill is increased by 5% compared to mix 1, the maximum compaction curve (MCC) is reduced by 19%, and dry density decreases by 5.7% in the ratio of 0.3 for maximum moisture content to dry density. The blue line symbolizes the normalized curve of the real-time plot of the actual results of the test (Bai et al., 2020). Figure 4 presents a regularized paraboli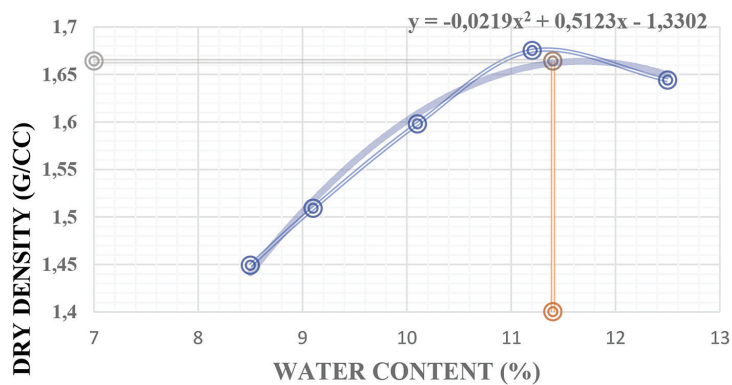c curve, displaying the moisture content at 11.4% and dry density at 1.93 g/cc for the mix proportion of 70% pond ash, 20% RAP, and 10% backfill soil. Figure 4 illustrates the symmetry of the averaged curve plot

moisture content at 11.4% and dry density at 1.66 g/cc for the mix proportion of 60% pond ash, 20% RAP, and 20% backfill soil. The dry side shows maximum plotting variables, which are significant for road pavement conditions. The MCC does not show any changes from mix type 3 to mix type 4, emphasizing that the optimum mix for road pavement is suitable for moderate traffic flow (Vivekananthan et al., 2023). The solid blue line symbolizes the normalized curve of the real-time plot of the actual results of the test, which is plotted in a translucent line. Figure 6 presents a

$$y = -0.0156x^2 + 0.3469x - 0.0029$$
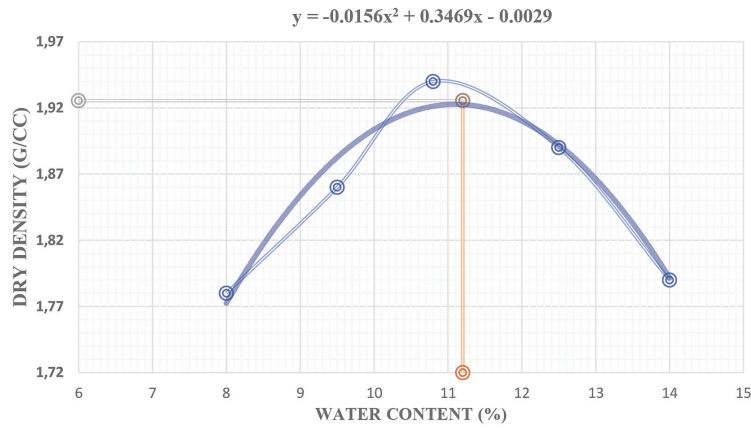
Figure 4. Dry density vs. moisture content for sample mix type 3

$$y = -0.0219x^2 + 0.5123x - 1.3302$$

Figure 5. Dry density vs. moisture content for sample mix type 4

$$y = -0.0014x^2 + 0.0372x + 1.679$$
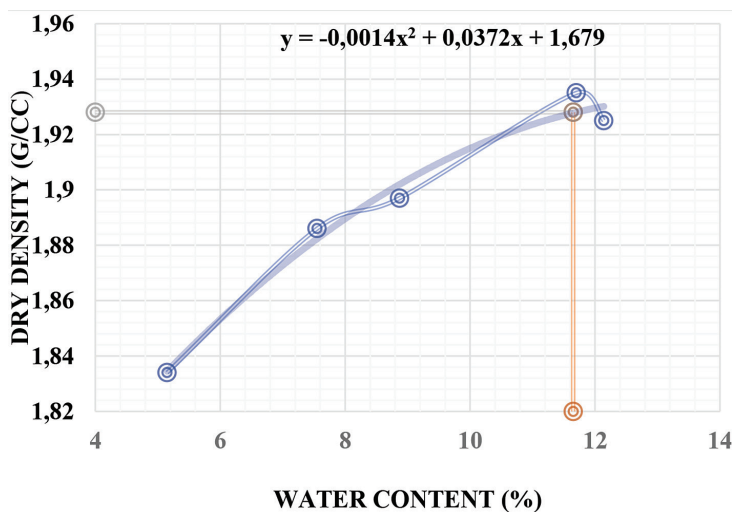
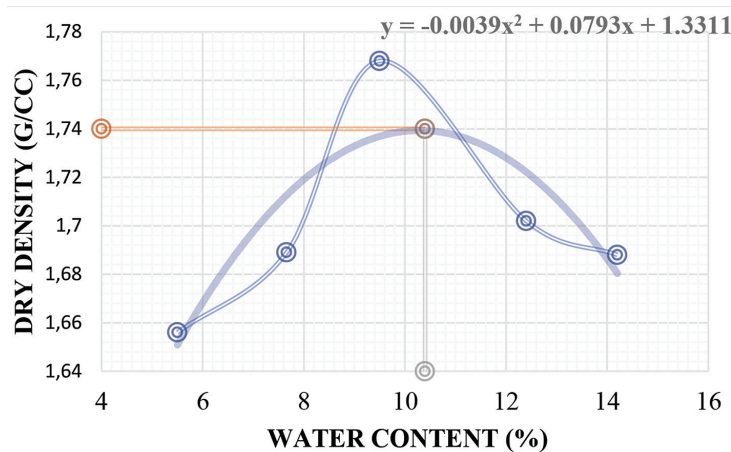**Figure 6.** Moisture content vs. dry density for sample mix type 5

Figure 7. Moisture content vs. dry density for sample mix type 6

regularized parabolic curve, displaying the moisture content at 11.65% and dry density at 1.928 g/cc for the mix proportion of 50% pond ash, 30% RAP, and 20% backfill soil (Mohammadinia et al., 2015). The dry side shows maximum plotting variables, which are significant for road pavement conditions. However, a change in the MCC from mix type 4 to mix type 5 and a sudden dip in the wet portion indicate the vulnerability of soil compaction for this mix. Therefore, this mix cannot be preferred for road pavement. Figure 7 illustrates a normalized quadratic equation formed for a parabolic curve, which displays the moisture content at 10.4% and dry density at 1.74 g/cc for the mix proportion of 40% pond ash, 30% RAP, and 30% backfill soil (Soleimanbeigi and Edil 2015). The actual curve and normalized curve indicate a compaction differential due to the major portions being RAP and backfill soil, which results in porous formation due to the reduced presence of infill material (i.e., fly ash). Consequently, mix type 5 marks the end of the iteration process (De Lira et al., 2015; Arun et al., 2017).

CONCLUSIONS

The engineering parameters were determined for individual materials, such as pond ash, RAP, and backfill soil. The assessed characteristics demonstrate that the replacing materials resemble the properties of soil, leading to the decision to select these materials as sub-base and subgrade fill materials. Optimum moisture content and relative density were established for different proportions of the mixing matrix, with pond ash

varying from 90 to 40%, RAP from 5 to 30%, and local soil backfill from 5 to 30%. The strength of RAP aggregate as a structural pavement component is most pronounced when stabilized with cement, rather than blended in RAP. The sample moisture content and dry density for different proportions were identified using standard and modified proctor tests. The test results of the standard proctor test were depicted in graphical representation. The main objective of this study was to determine the optimum value of moisture content and maximum dry density of the mixed proportions of PA, RAP, and natural backfill soil. In the experimental study, MDD and OMC increase with the decreasing mix proportions of PA from 90 to 50%, RAP from 50 to 30%, and natural backfill soil from 50 to 20%.

As a result of treating the RAP materials for reuse by emulsification, the hygroscopic water bond property is enhanced due to the viscous bitumen adhering to the coarse aggregates, which results in an increase in MCC with the increment of RAP until the optimum mix is reached. This reveals the optimum usage of waste materials in the construction of roadways, particularly in the sub-base and wearing courses. Upon interpretation, the OMC and MDD were found to be 11.65% and 1.928 g/cc, respectively, for the mix of 50%:30%:20%, which is closer to conventional limitations according to the Indian Road Congress.

Consequently, the mix ratio of 0.5:0.3:0.2 can be replaced as optimum and applied for field works on a trial-and-error basis. The current research assessed the use of materials in the sub-base to achieve maximum dry density and optimum moisture content using pond ash and reclaimed

asphalt pavement materials in road construction. The extension of the work is to be carried out for various additional proportions in the future. Future research will focus on the recycling of materials and cost analysis to effectively demonstrate the cost of alternative materials when compared to conventional materials.

Acknowledgments

REFERENCES

1. Dager, C.H., Morro, R.H., Hubler, J.F. and Sample-Lord, K.M., 2023. Review of Geotechnical Properties of Reclaimed Asphalt Pavement for Reuse in Infrastructure. Geotechnics, 3(1), 21–42.

2. Qin, Z., Jin, J., Liu, L., Zhang, Y., Du, Y., Yang, Y. and Zuo, S., 2023. Reuse of soil-like material solidified by a biomass fly ash-based binder as engineering backfill material and its performance evaluation. Journal of Cleaner Production, 402, 136824.

3. Zhang, Z., Li, W. and Yang, J., 2021. Analysis of stochastic process to model safety risk in construction industry. Journal of Civil Engineering and Management, 27(2), 87–99.

4. Zhang, X. and Yang, D., 2022. Experiment of static creep behavior of aggregate-asphalt interfaces. Journal of Computational Methods in Sciences and Engineering, 22(5), 1809–1818.

5. Barmade, S., Patel, S. and Dhamaniya, A., 2022. Performance evaluation of stabilized reclaimed asphalt pavement as base layer in flexible pavement. Journal of Hazardous, Toxic, and Radioactive Waste, 26(1), 04021051.

6. Gupta, D. and Kumar, A., 2016. Strength characterization of cement stabilized and fiber reinforced clay–pond ash mixes. International Journal of Geosynthetics and Ground Engineering, 2, 1–11.

7. Rout, M.D., Sahdeo, S.K., Biswas, S., Roy, K. and Sinha, A.K., 2023. Feasibility study of reclaimed asphalt pavements (RAP) as recycled aggregates used in rigid pavement construction. Materials, 16(4), 1504.

8. Plati, C., Tsakoumaki, M. and Gkyrtis, K., 2022. Physical and Mechanical Properties of Reclaimed Asphalt Pavement (RAP) Incorporated into Unbound Pavement Layers. Applied Sciences, 13(1), 362.

9. Liu, C., Cui, J., Zhang, Z., Liu, H., Huang, X. and Zhang, C., 2021. The role of TBM asymmetric tail-grouting on surface settlement in coarse-grained soils of urban area: Field tests and FEA modelling. Tunnelling and Underground Space Technology, 111, 103857..

10. Liu, S., Hou, J., Suo, C., Chen, J., Liu, X., Fu, R. and Wu, F., 2022. Molecular-level composition of dissolved organic matter in distinct trophic states in Chinese lakes: implications for eutrophic lake management and the global carbon cycle. Water Research, 217, 118438.

11. Zhang, J., Zhang, A., Li, J., Li, F. and Peng, J., 2019. Gray correlation analysis and prediction on permanent deformation of subgrade filled with construction and demolition materials. Materials, 12(18), 3035.

12. Kaseer, F., Arámbula-Mercado, E. and Martin, A.E., 2019. A method to quantify reclaimed asphalt pavement binder availability (effective RAP binder) in recycled asphalt mixes. Transportation Research Record, 2673(1), 205–216.

13. Sarkar, R. and Dawson, A.R., 2017. Economic assessment of use of pond ash in pavements. International Journal of Pavement Engineering, 18(7), 578–594.

14. Pasandín, A.R. and Pérez, I., 2013. Laboratory evaluation of hot-mix asphalt containing construction and demolition waste. Construction and Building Materials, 43, 497–505..

15. Muniamuthu, S., Kumar, K.S., Raja, K. and Rupesh, P.L., 2022. Dynamic characterization of hybrid composite based on flax/E-glass epoxy composite plates. Materials Today: Proceedings, 59, 1786–1791.

16. Yang, Z., Xu, J., Feng, Q., Liu, W., He, P. and Fu, S., 2022. Elastoplastic analytical solution for the stress and deformation of the surrounding rock in cold region tunnels considering the influence of the temperature field. International Journal of Geomechanics, 22(8), 04022118.

17. Seferoğlu, A.G., Seferoğlu, M.T. and Akpınar, M.V., 2018. Investigation of the effect of recycled asphalt pavement material on permeability and bearing capacity in the base layer. Advances in civil engineering, 2018, 1–6.

18. Kumar, K.S., Alqarni, S., Islam, S. and Shah, M.A., 2024. Royal Poinciana Biodiesel Blends with 1-Butanol as a Potential Alternative Fuel for Unmodified Research Engines. ACS Omega.

19. Al-Ghurabi, S.B. and Al-Humeidawi, B.H., 2021. May. Comparative evaluation for the effect of particles size of reclaimed asphalt pavement (RAP) on the properties of HMA. In Journal of Physics: Conference Series, 1895(1), 012025. IOP Publishing.

20. Pradhan, S.K. and Biswal, G., 2022. Utilization of reclaimed asphalt pavement (RAP) as granular sub-base material in road construction. Materials Today: Proceedings, 60, 288–293.

21. Edeh, J.E., Joel, M. and Abubakar, A., 2019.

Sugarcane bagasse ash stabilization of reclaimed asphalt pavement as highway material. International Journal of Pavement Engineering, 20(12), 1385–1391.

22. Tarsi, G., Tataranni, P. and Sangiorgi, C., 2020. The challenges of using reclaimed asphalt pavement for new asphalt mixtures: A review. Materials, 13(18), 4052.

23. Kumar, K.S., Yogesh, P., Vemulakonda, H.N. and Kumar, K.H., 2023. Performance, combustion and emissions characteristics of palm biodiesel blends in CI engines. Materials Today: Proceedings.

24. Antunes, V., Neves, J. and Freire, A.C., 2021. Performance assessment of Reclaimed Asphalt Pavement (RAP) in road surface mixtures. Recycling, 6(2), 32.

25. Gottumukkala, B., Kusam, S.R., Tandon, V. and Muppireddy, A.R., 2018. Estimation of blending of rap binder in a recycled asphalt pavement mix. Journal of Materials in Civil Engineering, 30(8), 04018181.

26. Ghanizadeh, A.R., Rahrovan, M. and Bafghi, K.B., 2018. The effect of cement and reclaimed asphalt pavement on the mechanical properties of stabilized base via full-depth reclamation. Construction and Building Materials, 161, 165–174.

27. Sunil Kumar, K., Muniamuthu, S. and Tharanisrisakthi, B.T., 2022. An investigation to estimate the maximum yielding capability of power for mini venturi wind turbine. Ecological Engineering & Environmental Technology, 23.

28. Elkashef, M., Podolsky, J.H., Christopher Williams, R., Hernandez, N. and Cochran, E.W., 2019. Using viscosity models to predict the properties of rejuvenated reclaimed asphalt pavement (RAP) binders. Road Materials and Pavement Design, 20(sup2), S767–S779.

29. Saravanan, A., Sudharsan, G., Suresh, P., Salaisargunan, S.P., Anandhi, S. and Kumar, K.S., 2024. Performance Study on a High-Strength Extruded Magnesium Alloy Van Frame Using FEA. Strength of Materials, 1–13.

30. Bishnoi, D., 2023. Pressure exertion and heat dissipation analysis on uncoated and ceramic (Al2O3, TiO2 and ZrO2) coated braking pads. Materials Today: Proceedings, 74, 774–787.

31. Adhikari, S., Khattak, M.J. and Adhikari, B., 2020. Mechanical characteristics of Soil-RAP-Geopolymer mixtures for road base and subbase layers. International Journal of Pavement Engineering, 21(4), 483–496.

32. Bai, B., Bai, F., Nie, Q. and Jia, X., 2023. A high-strength red mud–fly ash geopolymer and the implications of curing temperature. Powder Technology, 416, 118242.

33. Srimanickam, B. and Kumar, S., 2021. Drying investigation of coriander seeds in a photovoltaic thermal collector with solar dryer. Int. J. Mech. Eng. Technol, 14, 659–668.

34. Arshad, M. and Ahmed, M.F., 2017. Potential use of reclaimed asphalt pavement and recycled concrete aggregate in base/subbase layers of flexible pavements. Construction and Building Materials, 151, 83–97.

35. Vivekananthan, V., Vignesh, R., Vasanthaseelan, S., Joel, E. and Kumar, K.S., 2023. Concrete bridge crack detection by image processing technique by using the improved OTSU method. Materials Today: Proceedings, 74, 1002–1007.

36. Mohammadinia, A., Arulrajah, A., Sanjayan, J., Disfani, M.M., Bo, M.W. and Darmawan, S., 2015. Laboratory evaluation of the use of cement-treated construction and demolition materials in pavement base and subbase applications. Journal of materials in civil engineering, 27(6), 04014186.

37. Soleimanbeigi, A. and Edil, T.B., 2015. Compressibility of recycled materials for use as highway embankment fill. Journal of Geotechnical and Geoenvironmental Engineering, 141(5), 04015011.

38. Karthikeyan, N.K., Arun, S., Mohan, G.S. and Kumar, S., 2017. Structural analysis of exhaust manifold for 1500 Hp engine. International Journal of Mechanical Engineering and Technology, 8(3), 379–387.

39. De Lira, R.R., Cortes, D.D. and Pasten, C., 2015. Reclaimed asphalt binder aging and its implications in the management of RAP stockpiles. Construction and Building Materials, 101, 611–616.

40. Arun, S., Nagoorvali, S.K., Kumar, K.S. and Mohan, G.S., 2017. Automation of main bearing bolt and cap loosening machine for automobile crankshaft. Int J Mech Eng Technol, 8, 41–49.